Water Resour Manage (2014) 28:1449–1462
DOI 10.1007/s11269-014-0565-7

Impact of Climate Change on Mediterranean Irrigation Demand: Historical Dynamics of Climate and Future Projections

I. García-Garizábal · J. Causapé · R. Abrahao · D. Merchan

Received: 19 December 2013 / Accepted: 18 February 2014 /
Published online: 14 March 2014
© Springer Science+Business Media Dordrecht 2014

Abstract Global warming is causing important changes in climate conditions, which must be studied in detail and locally in those zones where irrigated agriculture is developed—the major consumer of water worldwide. This study proposes the climatic characterization of a historical series (1971–2000) and its future projections (2011–2099) for an Irrigation District located in the Middle Ebro Valley (Spain), for three different scenarios: low, medium, and high global emission levels of greenhouse gases. Analysis of historical series reveals a significant increase in reference evapotranspiration (3.3 mm/year^2; 2.4 ‰) along with a decrease in precipitation (2.5 mm/year^2; 5.6 ‰). A comparison was carried out between real historical data and the scenarios produced by the climate models and it was observed that the most adequate climate model to predict climate in the study zone is MPI-ECHAM5. For the XXI century, MPI-ECHAM5 predicts cyclic climate trends but with a general increment in aridity, which intensifies according to the scenario chosen. Changes in climate are affecting agriculture doubly, since evapotranspiration requirements increase at the same time that water resources decrease. These effects are felt especially in irrigated agriculture, since the growing cycles of the main crops coincide with the months most affected by climate change.

Keywords Agriculture · Evapotranspiration · Precipitation · Temperature · Model · Trend

1 Introduction

Irrigated agriculture allows for the stable supply of food and raw materials at the expense of the consumption of 75 % of the water resources used by mankind (FAO 2002, 2003). Climate variables such as temperature (directly related to evapotranspiration), and precipitation play an essential role in the water requirements of crops and therefore are the main climate variables that affect irrigation.

I. García-Garizábal (✉) · J. Causapé · D. Merchan
Geological Survey of Spain (IGME), C\ Manuel Lasala 44, 9°B. 50.006, Zaragoza, Spain
e-mail: ikerggarizabal@gmail.com

R. Abrahao
Center of Alternative and Renewable Energy, Department of Renewable Energy Engineering, Federal University of Paraiba, Cx Postal 5115, 58051-900 João Pessoa, Paraíba, Brazil

The Intergovernmental Panel on Climate Change (IPCC 2007) remarked that global warming due to the emission of greenhouse gases is a verified fact through which important changes are predicted in many climate variables. Among these, temperature stands out, with an increasing trend of 0.74 °C between 1901 and 2005, and precipitation, with wide spatial variability but general increases in northern regions and decreases in southern regions.

IPCC highlights the necessity of establishing adaptation and mitigation measures against climate change, although due to the complexity of the Earth system, it is impossible to detail such actions at a global level and it is necessary to carry out detailed studies at local scales.

With the purpose of studying the impact of climate dynamics and developing management strategies against climate change, multiple research centers have developed models capable of predicting climate. Websites such as the Canadian Climate Change Scenarios Network (CCCS N, www.cccsn.ec.gc.ca/) compile these models and make them available to potential users.

The climate models are oriented towards the creation of future climate scenarios for the evaluation of management strategies, but it is very important to analyze each model individually, as at a local scale the different models and scenarios can result in different outcomes for the same study zone. Nevertheless, all models coincide in that arid and semiarid regions are more sensitive to climate changes than humid regions (IPCC 2008).

In the Iberian Peninsula, several studies have analyzed the dynamics of temperature (De Luis et al. 2007; Del Río et al. 2011, 2012; El Kenawi et al. 2012; Espadafor et al. 2011; González-Aparicio and Hidalgo 2011; Lopez-Moreno et al. 2011; Saz Sánchez et al. 2007; Ramos et al. 2012) and of precipitation (De Luis et al. 2000, 2007, 2009, 2010, 2011; Gonzalez-Hidalgo et al. 2009, 2010, 2011; Lopez-Moreno et al. 2011; Palatella et al. 2010; Ramos et al. 2012; Saz Sánchez et al. 2007; Vicente-Serrano and López-Moreno 2006; Vicente-Serrano and Cuadrat-Prats 2007) for the last 60 years, demonstrating increasing trends for temperature and decreasing trends for precipitation, much more pronounced than those calculated for global studies (IPCC 2007).

Although the aforementioned studies contribute with valuable information on the behaviour and climate trends, the authors themselves recommend the elaboration of more local studies in order to deepen knowledge on the problematic of each zone and to plan concrete actions (Gonzalez-Hidalgo et al. 2011; Vicente-Serrano and Cuadrat-Prats 2007). This fact must be taken into account especially in the Mediterranean environment (IPCC 2008) and concretely in the Ebro basin, which is pointed out as one of the Mediterranean hydrological basins most affected by climate change (Palatella et al. 2010; Sanchez-Arcilla et al. 2011). Previous studies already demonstrated the high spatial variability in the historical trends of climate variables in the Ebro basin (De Luis et al. 2007, 2009; Gonzalez-Hidalgo et al. 2009, 2011; Lopez-Moreno et al. 2011).

This study analyzes the consequences of climate change and its effects on the main climatic parameters of an agricultural area of the Middle Ebro Valley. This study aims at characterizing the dynamics of climate, selecting the most adequate model for the study zone, and analyzing the projections for three hypothetical scenarios with different climate change intensities.

2 Methodology

2.1 Climate Information of the Study Area

The study area corresponds to the Irrigation District n° V of Bardenas (15,500 ha), located on the left margin of the Middle Ebro Valley (Fig. 1).

In the Irrigation District Center there is a climatic station of the State Meteorological Agency (*In Spanish: AEMET*) with historical registries of temperature (T) and precipitation

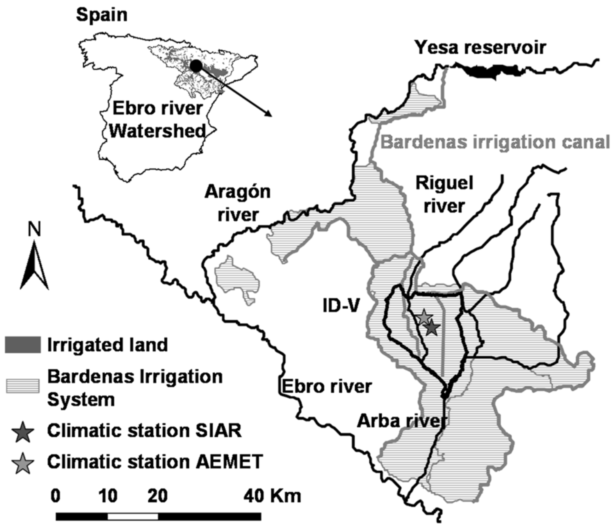

Fig. 1 Irrigation District n° V of Bardenas (CR-V) and its location in the Ebro river basin. Location of the climatic stations utilized in the study

(P) since 1970. This is a homogeneous series that has been widely tested (El Kenawi et al. 2011; Vicente-Serrano et al. 2010). The evapotranspiration daily series was obtained from these data by applying the Hargreaves method ($ET_{0\ H}$; Allen et al. 1998).

In 2005 another agroclimatic station of the Integrated Irrigation Advisory Service (SIAR network) began operating, which allows for obtaining reference evapotranspiration through the Penman-Monteith method ($ET_{0\ PM}$; Allen et al. 1998), which is the most precise method according to tests carried out in lysimeters (Martínez-Cob and Tejero-Juste 2004).

For the period between 2005 and 2009, with data from both climatic stations, a significant relationship was found between the two methods used to estimate reference evapotranspiration. This relationship was utilized to correct the historical ET_0 to the most precise method, resulting in the historical ET_0 daily series through Penman-Monteith.

$$ET_{0\ PM}[\mathrm{mm/day}] = 0.48{\cdot}ET_{0\ H}[\mathrm{mm/day}] + 0.292 \quad (n = 1675; p < 0.001) \tag{1}$$

2.2 Climatic Characterization

Given that the Intergovernmental Panel on Climate Change recommends minimum study periods of 30 years and the climate models available on the internet (www.cccsn.ec.gc.ca/) provide data between 1971 and 2000, this was the period selected to characterize the climate historical dynamics of the study zone.

The Aridity Index (AI; UN 2011) was determined using annual precipitation and reference evapotranspiration data, providing classifications for the climate of arid zones: hyper-arid deserts (AI<0.05), arid (0.05<AI<0.20), semi-arid (0.20<AI<0.50) and sub-humid arid (0.50 <AI<0.65).

$$AI = \frac{P}{ET_0} \tag{2}$$

Regarding pluviometry, the years pertaining to the data series were classified as dry, normal or rainy years according to the Standardized Precipitation Index (SPI; McKee et al. 1993; McKee et al. 1995). This index is considered to be the best climatic indicator to identify drought-rain periods (Keyantash and Dracup 2002) and has been utilized in several studies throughout the world with satisfactory results (Bonaccorso et al. 2003; Burgueno et al. 2010; Capra et al. 2013; Domonkos 2003; Hayes et al. 1999; Lloyd-Hughes and Saunders 2002; Loukas and Vasiliades 2004; Rouault and Richard 2003; Bordi et al. 2004; Turkes and Tatli 2009; Vicente-Serrano and López-Moreno 2006; Zargar et al. 2014).

To this end, precipitation data are adjusted to a Pearson III distribution (Guttman 1999). Once adjusted, the resulting precipitation series are transformed into a normal distribution (0,1), in such a way that the normalized value indicates the probability corresponding to a Pearson III distribution. The positive values of the distribution always indicate a precipitation superior to the average, while negative values indicate inferior precipitation than the average, and normal periods are defined by SPI values between −1.0 and 1.0. Once these values are exceeded, the analyzed period is defined as "rainy" or "dry".

The Precipitation Concentration Index (PCI; Oliver 1980) was also calculated to define rain distribution, and has been satisfactorily tested in many regions (Apaydin et al. 2006; De Luis et al. 2000, 2010, 2011; Elagib 2011; Martins et al. 2012; Pizarro et al. 2008; Raziei et al. 2008). PCI is calculated as follows:

$$PCI_{year} = 100 \cdot \frac{\sum_{i=1}^{12} p_i^2}{\left(\sum_{i=1}^{12} p_i\right)^2} \tag{3}$$

being p_i the amount of rain corresponding to month i.

A value of PCI under 10 indicates a uniform rain distribution, values between 11 and 20 mark a seasonal character of rain, while values over 20 define climates with a substantial monthly variation in precipitation.

Finally, trend analysis (τ) was carried out to analyze the dynamics of climate. Given the non-normal character of the climate data series (ET_0 and P), the Mann-Kendall range test was applied (Kendall 1975; Mann 1945) and the Sen's slope was calculated (Sen 1968) as a trend quantifier. The weight of each trend within its period was obtained by dividing the trend by the average of the period in which it was obtained.

In order to smooth the series and improve visualization of the temporal dynamics, some graphs were elaborated with moving averages (Sneyers 1992). In this sense, De Luis et al. (2000) calculated the moving averages for the Mediterranean area for the last 9 years.

2.3 Climate Change Projections

Selection of the climate model that better fits the conditions of the study zone started from an initial analysis carried out by Errasti et al. (2011), which establishes—after analyses of 24 models developed by 16 institutions—that climate models MIROC3.2-HIRES, MPI-ECHAM5, GFDL-CM2.1, BCCR-BCM2.0 and UKMO-HADGEM1 are the most adequate for the Iberian Peninsula. These models start from historical series of temperature and precipitation for the period 1971–2000, and are capable of generating projections for the period 2011–2099 under the three scenarios proposed by IPCC (2007).

All scenarios are equally valid, with no allocation of probabilities to become reality. The three scenarios proposed by the models were taken from the four families proposed by IPCC, which describe relationships between the distinct influences of greenhouse gas emissions and aerosols as well as the dynamics during the XXI century. Each dynamics line represents a demographic, social, economic, technological, and environmental change.

– *Dynamic line and scenario family A1:* describes a future world with a rapid economic growth, a world population that reaches a maximum value mid-century and decreases a posteriori, and a fast introduction of new, more efficient technologies. The family of scenarios A1 is developed in three groups that describe alternative directions for technological changes in the energy system: intensive use of fossil fuels (A1F1), use of non-fossil fuels (A1T), and balanced used of all types of fuels and sources (A1B).
– *Dynamic line and scenario family A2:* describes a very heterogeneous world with a global population in continuous growth. The economic development is oriented towards regions, and economic growth per inhabitant as well as technological changes are more fragmented and slow than in other dynamic lines.
– *Dynamic line and scenario family B1:* describes a convergent world with a balanced population, such as in dynamic line A1, but with fast changes in economic structures, oriented towards information and service economy, along with a less intensive utilization of materials and introduction of clean technologies with an effective use of resources.
– *Dynamic line and scenario family B2:* describes a world where local solutions to economic, social and environmental sustainability prevail, with a progressive increase of world population, although at a slower rate than A2, with intermediate economic development levels.

Most of the models proposed by Errasti et al. (2011) contemplate the B1 scenarios, considered as "low", A1B, considered as "medium/intermediate", and A2, considered as "high" in greenhouse gas emissions. These three scenarios have been chosen to analyze the future dynamics of climate (2011–2099). Starting from the daily temperature values provided by the models, the reference evapotranspiration was estimated according to the Hargreaves method, followed by a correlation to Penman-Monteith.

The selection of the most adequate climate model was made after comparisons between historical averages and trends (1970–2000) regarding future projections provided by the models (2001–2099). This hypothesis has already been employed by Moratiel et al. (2010) to elaborate climate change projections for the Iberian Peninsula, and is in accordance with the proposal of stable trends (IPCC-TGICA 2007; Milly et al. 2005) and even with increasing trends (Milly et al. 2005) in calibration/validation parameters for climate change scenarios. In this sense, when choosing the model, temperature trends prevailed over precipitation, resulting in a less complex parameter calculation in the climate change projections (Errasti et al. 2011; IPCC-TGICA 2007).

3 Results and Discussion

3.1 Historical Climate Characterization

According to the aridity index, the climate of the study zone is classified as semi-arid (AI=0.33), with a variability that comprehends extreme years with aridity indices between 0.45 and 0.19 (already considered as arid: AI≤0.2).

Following the climate parameters most important to irrigation, ET_0 presented an average annual value of 1,384 mm with low interannual variability (VC=3 %; Fig. 2). Nevertheless, ET_0 presented cycles with maximums in Summer, when 44 % of the annual ET_0 accumulated, and minimums in Winter, with only 9 % of the annual ET_0 (Fig. 3).

Average precipitation throughout the period 1971–2000 was 448 mm/year, with a well-defined interannual variability (VC=20 %), characteristic of the Mediterranean climate (De Luis et al. 2000, 2011; Philandras et al. 2011; Ramos 2001; Saz Sánchez et al. 2007), with dry years (255 mm) and humid years (up to 600 mm; Fig. 2).

According to the Standardized Precipitation Index, 13 % of the years were classified as "humid" and 24 % were classified as "dry". Moreover, rain presents a very pronounced seasonality with an average Precipitation Concentration Index of 14 for the entire study period. Occasionally, a year can exceed a PCI of 20, defining a climate with substantial monthly variability.

The highest contributions of rain are produced in Autumn and Spring, which account for 58 % of annual precipitation and a very variable annual distribution since PCI oscillates between 8 and 24. The highest values of precipitation were produced in May and April (12.3 % and 10.5 % of the annual total) while the lowest values were registered in July and August (5.1 % and 5.3 % of the annual total; Fig. 3).

Therefore Summer registered the periods of lowest precipitation, coinciding with the highest ET_0. This fact is of great importance because it results in indispensable irrigation to satisfy the hydric demands of the main crops developed in the zone (García-Garizábal and Causapé 2010; García-Garizábal et al. 2011).

Analysis of the historical series (1971–2000) detected a significant increment of 3.3 mm/year^2 in ET_0 (2.4 ‰; Fig. 2), although with some variability in trends throughout the year, which in many cases, when considering a monthly scale, cease to be statistically significant (Fig. 3).

It is remarkable that the highest increases in evapotranpiration occurred in Spring (2.4 mm/season·year; 6.3 ‰) and that in comparison with the general annual increase, Autumn registered a decrease of -0.3 mm/season·year (1.0 ‰). The highest ET_0 increase

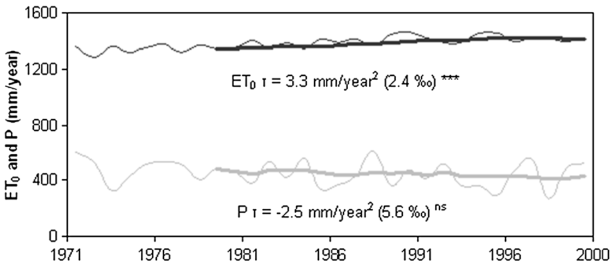

Fig. 2 Annual dynamics of reference evapotranspiration (ET_0) and precipitation (P) [9-year moving average shown in continuous line] in the study area for the period 1971–2000. Absolute trend (τ; mm/year2) and per thousand (‰). Statistical significance: ns = Non significant; + = p<0.1; * = p<0.05; ** = p<0.01; *** = p<0.001

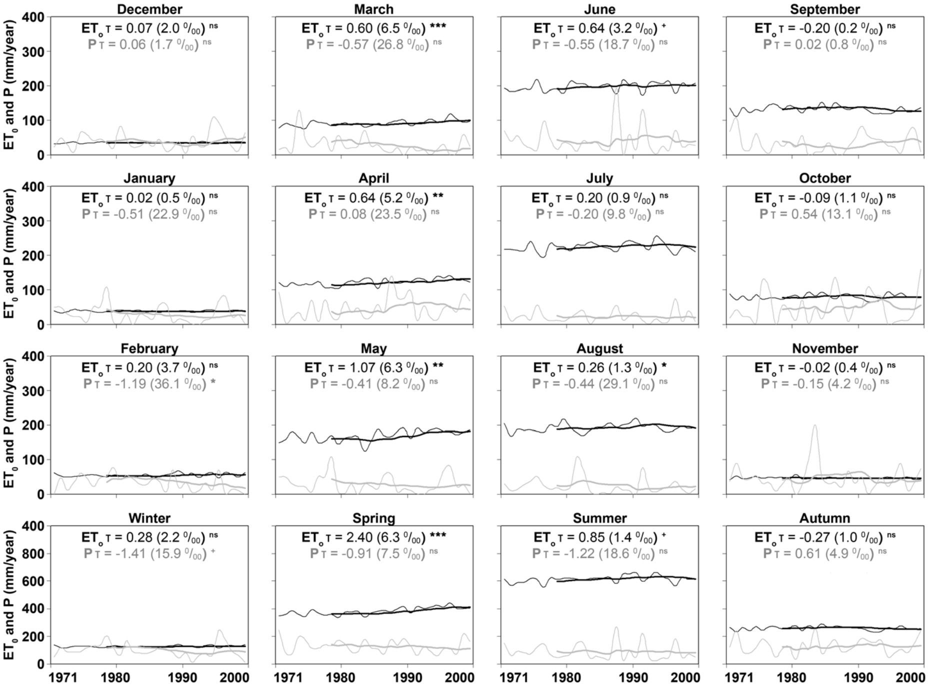

Fig. 3 Seasonal and monthly dynamics of reference evapotranspiration (ET_0) and precipitation (P) [9-year moving average shown in continuous line] in the study area for the period 1971–2000. Absolute trend (τ; mm/year2) and per thousand (‰). Statistical significance: ns = Non significant; + = $p<0.1$; * = $p<0.05$; ** = $p<0.01$; *** = $p<0.001$

rate was registered in May (1.1 mm/month·year; 6.3 ‰) and the most pronounced decrease was recorded in September (-0.2 mm/month·year; 0.2 ‰).

Therefore, evapotranspiration variation rates are of the same order or inferior to those found in the southeastern Iberian Mediterranean by Espadafor et al. (2011), with increment rates of 0.4–3.7 mm/year^2.

Regarding precipitation trends, during the period 1971–2000 there was a decrease of 2.5 mm/year^2 in precipitation (5.6 ‰; Fig. 2). Although this trend was not statistically significant ($p>0.1$), the trend obtained with 9-year moving averages was statistically significant, smoothing the series ($p<0.001$).

As occurred for ET_0, the slopes obtained throughout the year are not homogeneous. Negative trends were seasonally detected for precipitation in Winter, Summer and Spring, while for Autumn an increase in precipitation was detected (Fig. 3). Monthly, the most pronounced decrease rates in precipitation were registered in February (−1.2 mm/month·year; 36.1 ‰) while April was the month with highest increase (1.0 mm/month·year; 23.5 ‰).

The amplitude of the data series allows for the distinction of months in which, although there is a general monotonic trend, ascendant and descendant intervals appear (Gonzalez-Hidalgo et al. 2010), easily observable after smoothing the monthly and seasonal precipitation registries (Fig. 3).

The rates obtained were of the same order of those found in other areas of the Ebro Valley and of the Mediterranean Iberian environment (De Luis et al. 2007, 2009; Gonzalez-Hidalgo et al. 2010; Lopez-Moreno et al. 2011; Saz Sánchez et al. 2007), although the trends estimated in these studies show a great spatial variability since relatively close zones present trends with opposite signs, highlighting the value of these studies at local scale.

3.2 Climate Models

The five models selected by Errasti et al. (2011) as being the most adequate for the Iberian Peninsula environment provide, for the different greenhouse gas emission scenarios, an ample range of temperature and precipitation trends, associated with a higher complexity embedded in its determination (Errasti et al. 2011). Nevertheless, all combinations of the model-scenario predict positive trends for temperature and negative trends for precipitation (Table 1). Except for model UKMO-HADGEM1, in the case of precipitation, the models always predict higher increments of temperature and decreases in precipitation in the models with higher emissions.

According to the positive trend observed, for all model-scenario combinations the average predicted temperature is higher than the historical average. In opposition, for precipitation, only model MPI-EHCAM5 in its three scenarios predicts annual average precipitation lower than the historical, in accordance with its historical and predicted negative trends (Table 1).

Additionally, models such as UKMO-HADGEM1 or BCCR-BCM2.0 provide, even for high emission scenarios, inferior temperature trends than the historical, a situation that a priori is not expected with an increase in emissions to the atmosphere.

In this sense, it seems appropriate to conclude that of the five models proposed by Errasti et al. (2011), model MPI-EHCAM5 is the most adequate for the study zone herein explored.

Table 1 Average and trend values of temperature (T) and precipitation (P) for the historical series (1971–2000) and projections (2011–2099) of the five models proposed by Errasti et al. (2011) in low-, medium, and high-level scenarios of greenhouse gas emissions

Model	Scenario		T		P	
			°C/year	°C/year^2	mm/year	mm/year^2
Historical series	1971–2000		14.1	0.056***	448	−2.5^{ns}
MIROC3.2-HIRES	2011–2099	Low	16.9	0.036***	544	−0.6^{ns}
		Medium	17.5	0.057***	535	−1.1^{ns}
		High	–	–	–	–
UKMO-HADGEM1	2011–2099	Low	–	–	–	–
		Medium	16.7	0.043***	568	−2.2*
		High	16.8	0.052***	576	−1.2^{ns}
GFDL-CM2.1	2011–2099	Low	15.6	0.023***	687	−0.6^{ns}
		Medium	16.7	0.047***	581	−1.4^{ns}
		High	16.7	0.060***	600	−3.0**
MPI-ECHAM5	2011–2099	Low	15.9	0.038***	439	−1.6**
		Medium	16.7	0.056***	412	−1.9***
		High	16.6	0.063***	399	−2.2***
BCCR-BCM2.0	2011–2099	Low	15.5	0.018***	482	−0.8^{ns}
		Medium	15.9	0.038***	460	−1.0^{+}
		High	16.0	0.048***	456	−1.0^{+}

Statistical significance: ^{ns} = Non significant; $^{+}$ = $p<0.1$; * = $p<0.05$; ** = $p<0.01$; *** = $p<0.001$

3.3 Climate Projections

Increases in evapotranspiration and decreases in precipitation follow a progression from the historical registries until the low, intermediate, and high level emission scenarios in such a way that the aridity index varies between 0.32 in the historical registry and 0.27 in the predicted high-level emission scenario—i.e., more arid as the scenario becomes more aggressive (Table 2).

The annual variability of reference evapotranspiration also increases gradually from the historical series (VC=3 %) to the predicted high-level emission scenario (VC=6 %). Nevertheless, annual variability of precipitation increases abruptly from the historical series (VC=30 %) to the three predicted scenarios (VC=33–34 %), with slight differences among them.

Comparison of the Standardized Precipitation Index within the historical series shows that, for the three predicted scenarios, there is a 17 % increase in the years considered as extreme (dry+humid). Regarding the dynamics of the extreme years for the different projections, as the level of emissions is increased, the number of dry years increases and the number of humid years decreases (Table 2). The model predicts not only that less precipitation will occur, but also more irregularly.

As occurred for the historical series, the degree of statistical significance of climate trends is higher for reference evapotranspiration than for precipitation. In this sense the significance increases in the projections, although it decreases when discretizing the temporal analysis (Table 3).

The projections (2011–2099) of the three scenarios utilizing the MPI-EHCAM5 model provide lower rates than those obtained in the historical series, although the percentage and absolute evapotranspiration and precipitation rates increase according to the scenarios (increasing level of emissions). Therefore, between 2011 and 2099 the model predicts that the trends in the high-level emission scenario for reference evapotranspiration (2.7 mm/year^2; 1.9 ‰) and precipitation (−2.2 mm/year^2; 5.8 ‰) will exceed by 58 % and 38 %, respectively, the low-level emission scenario.

Generally, the seasonal trends offered by the model confirm the historical trends with the highest variation rates, both for evapotranspiration and precipitation, in Spring and Summer months. The results obtained present an indirect incidence on the irrigated agriculture of the study zone since the growing cycle of the crops coincides with the period most affect by climate change.

Table 2 Reference evapotranspiration (ET_0), precipitation (P), aridity index (AI) and standardized precipitation index (SPI) for the historical series regarding the own historical series (1971–2000) and the projections (2011–2099) of the low-, medium-, and high-level scenarios of greenhouse gas emissions. The variation coefficient is shown between brackets

Scenarios		Historical	Low (B1)	Medium (A1B)	High (A2)
ET_0	mm/year	1,384 (3 %)	1,458 (4 %)	1,488 (5 %)	1,486 (6 %)
P	mm/year	448 (20 %)	439 (34 %)	412 (33 %)	399 (34 %)
AI		0.32	0.30	0.28	0.27
Standardized precipitation index (SPI)					
Dry	%	24	30	38	40
Normal	%	63	46	46	46
Humid	%	13	24	16	13

Table 3 Absolute and percentage trends for reference evapotranspiration (ET_0; mm/year^2) and precipitation (P; mm/year^2) in the historical series (1971–2000) and projections of the MPI-EHCAM5 model (2011–2099) in the low-, medium-, and high- level scenarios for greenhouse gas emissions

Scenarios		Historical		Low (B1)		Medium (A1B)		High (A2)	
Period		ET_0	P	ET_0	P	ET_0	P	ET_0	P
Annual	mm/year^2	3.28*** (2.4‰)	−2.47^{ns} (5.6‰)	1.68*** (1.1‰)	−1.56** (3.7‰)	2.39*** (1.6‰)	−1.94*** (5.0‰)	2.75*** (1.9‰)	−2.19*** (5.8‰)
Winter	mm/season· year	0.28^{ns} (2.2‰)	−1.41^{+} (15.9‰)	0.04** (0.9‰)	−0.29^{ns} (3.2‰)	0.06*** (1.3‰)	−0.19^{ns} (2.2‰)	0.07*** (1.6‰)	−0.30^{+} (3.3‰)
Spring		2.40*** (6.3‰)	−0.91^{ns} (7.5‰)	0.20*** (1.3‰)	−0.31^{ns} (2.8‰)	0.27*** (2.0‰)	−0.60** (5.9‰)	0.30*** (2.2‰)	−0.65** (6.3‰)
Summer		0.85^{+} (1.4‰)	−1.22^{ns} (18.6‰)	0.25*** (1.1‰)	−0.42** (8.3‰)	0.38*** (1.7‰)	−0.57*** (10.5‰)	0.43*** (1.9‰)	−0.59*** (13.2‰)
Autumn		−0.27^{ns} (1.0‰)	0.61^{ns} (4.9‰)	0.08** (0.9‰)	−0.38^{ns} (3.3‰)	0.11*** (1.2‰)	−0.25^{ns} (2.5‰)	0.14*** (1.5‰)	−0.56* (5.8‰)
January	mm/month· year	0.02^{ns} (0.5‰)	−0.51^{ns} (22.9‰)	0.03* (0.7‰)	−0.08^{ns} (3.8‰)	0.04** (1.0‰)	−0.04^{ns} (1.9‰)	0.05*** (1.2‰)	−0.03^{ns} (1.5‰)
February		0.20^{ns} (3.7‰)	−1.19* (36.1‰)	0.04^{+} (0.8‰)	−0.14^{ns} (4.9‰)	0.08** (1.5‰)	−0.10^{ns} (3.2‰)	0.08** (1.5‰)	−0.20* (7.3‰)
March		0.60*** (6.5‰)	−0.57^{ns} (26.8‰)	0.13*** (1.4‰)	−0.08^{ns} (3.7‰)	0.17*** (1.8‰)	−0.12^{ns} (5.9‰)	0.20*** (2.1‰)	−0.11^{ns} (6.6‰)
April		0.64** (5.2‰)	0.08^{ns} (23.5‰)	0.18*** (1.4‰)	0.01^{ns} (0.3‰)	0.23*** (1.8‰)	−0.09^{ns} (2.8‰)	0.27*** (2.1‰)	−0.09^{ns} (2.8‰)
May		1.07** (6.3‰)	−0.41^{ns} (8.2‰)	0.25*** (1.4‰)	−0.16^{ns} (4.4‰)	0.37*** (2.0‰)	−0.21* (7.5‰)	0.38*** (2.1‰)	−0.19** (6.5‰)
June		0.64^{+} (3.2‰)	−0.55^{ns} (18.7‰)	0.23*** (1.1‰)	−0.11^{+} (5.9‰)	0.38*** (1.8‰)	−0.18** (10.1‰)	0.46*** (2.2‰)	−0.16* (8.5‰)
July		0.20^{ns} (0.9‰)	−0.20^{ns} (9.8‰)	0.30*** (1.2‰)	−0.06^{ns} (4.5‰)	0.41*** (1.7‰)	−0.15*** (13.6‰)	0.46*** (1.9‰)	−0.17*** (15.1‰)
August		0.26* (1.3‰)	−0.44^{ns} (29.1‰)	0.25*** (1.2‰)	−0.08^{+} (8.4‰)	0.37*** (1.8‰)	−0.08^{+} (8.4‰)	0.39*** (1.9‰)	−0.14*** (19.9‰)
September		−0.20^{ns} (0.2‰)	0.02^{ns} (0.8‰)	0.14** (1.0‰)	−0.24** (10.6‰)	0.18** (1.3‰)	−0.11^{ns} (4.9‰)	0.21*** (1.5‰)	−0.15* (7.4‰)
October		−0.09^{ns} (1.1‰)	0.54^{ns} (13.1‰)	0.08* (1.0‰)	−0.08^{ns} (2.4‰)	0.13** (1.5‰)	−0.06^{ns} (2.0‰)	0.14*** (1.6‰)	−0.10^{ns} (3.3‰)
November		−0.02^{ns} (0.4‰)	−0.15^{ns} (4.2‰)	0.04** (0.8‰)	−0.07^{ns} (2.3‰)	0.06*** (1.2‰)	−0.06^{ns} (2.0‰)	0.07*** (1.4‰)	−0.10^{ns} (3.6‰)
December		0.07^{ns} (2.0‰)	0.06^{ns} (1.2‰)	0.03** (1.7‰)	−0.02^{ns} (0.6‰)	0.05*** (1.3‰)	−0.07^{ns} (1.2‰)	0.05*** (1.4‰)	−0.06^{ns} (2.0‰)

Statistical significance: ^{ns} = Non significant; $^{+}$ = $p<0.1$; * = $p<0.05$; ** = $p<0.01$; *** = $p<0.001$

The absolute monthly rates of evapotranspiration and precipitation are statistically related in such a way that, as evapotranpiration increases more remarkably, the same occurs for the decrease in precipitation. The period with highest evapotranspirative demand will be doubly affected, since besides the increase in evapotranspirative demand there will also be a decrease in available water resources.

Moratiel et al. (2010) studied ET_0 dynamics and trends in Spain, and have also concluded that the most sensitive months to increases in ET_0 were May, June, July and August, while November, December and January were the least affected.

The results of the MPI-EHCAM5 model indicate that the climate trends will not be constant during the entire predicted series, but will occur in cycles. The three scenarios evolve relatively in parallel and when faced with the general trends described previously, present periods in which the rates are maximized, and periods with inverted trends (Fig. 4).

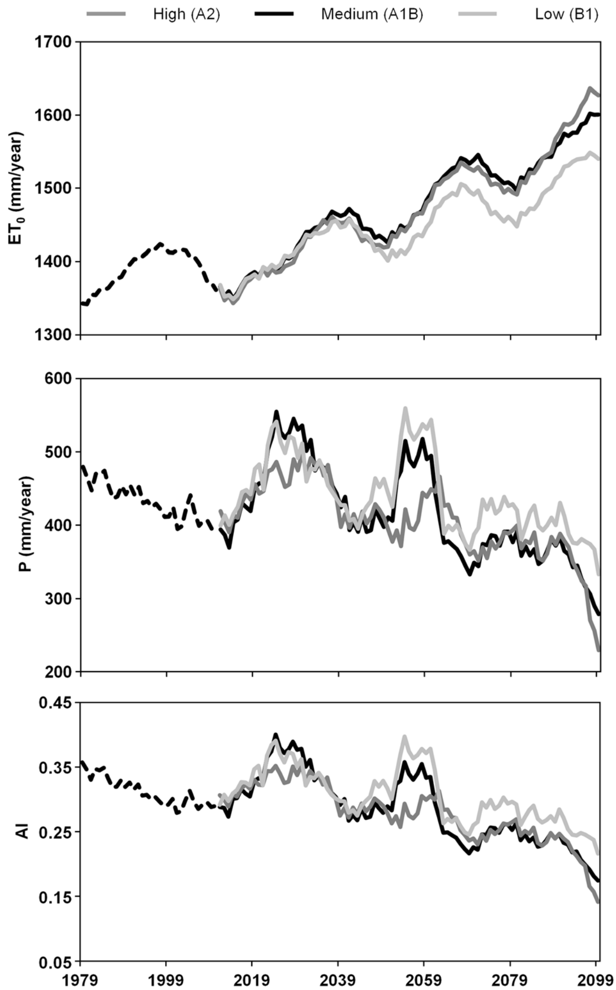

Fig. 4 Dynamics of the moving averages (last 9 years) of reference evapotranspiration (ET_0), precipitation (P) and aridity index (AI) between 1979 and 2099 with the climate projections of the MPI-EHCAM5 model for low-, medium-, and high-level scenarios for greenhouse gas emissions

Similarly to what occurred at a seasonal level, the aridity index is doubly affected due to the opposite trends in evapotranspiration and pluviometry. After relative increases throughout the predicted series, the general trend decreases in such a way that, at the end of the predicted series, climate can be characterized as arid (AI <0.1), in particular, when faced with intermediate- or high-level emission hypothetical scenarios for greenhouse gases.

4 Conclusions

Analysis of the historical series (1971–2000) of the Irrigation District n° V of Bardenas has highlighted the fact that reference evapotranspiration has increased (3.3 mm/year^2; 2.4 ‰) and precipitation has decreased (2.5 mm/year^2; 5.6 ‰), reflected at annual, seasonal, and monthly levels.

The climate models offer a wide variety of results, which is why tests at a local level with reference historical data are necessary. In this sense, the MPI-ECHAM5 model has been considered as the most adequate to carry out projections in the Irrigation District of Bardenas.

The results of the climate projections (2011–2099) of the MPI-ECHAM5 model for the Irrigation District of Bardenas continue to support the trends found in the historical series, with more pronounced climate changes according to the level of greenhouse gas emissions in the simulated scenario.

Although the dynamics of trends are not uniform, alternating maximum rate periods with others of inverted trends, the general trend results in an increase in the aridity level, with an arid climate being obtained at the end of the century (AI<0.20).

The evapotranspiration and precipitation trends are opposite, which affects irrigation agriculture doubly, as evapotranspiration requirements increase with a decrease of water resources, especially if the growing cycle of the crops is considered—which coincides with the period most affected by climate change.

Acknowledgments This work was supported within the framework of Project 2012/GA LC 016 of the Aragon Government and La Caixa, and also by the Geological Survey of Spain *(In Spanish: IGME*). Thanks are extended to Sergio M. Vicente-Serrano (IPE-CSIC) for facilitating the historical climate data for the study area.

References

Allen R, Pereira L, Raes D, Smith M (1998) Crop evapotranspiration. Guidelines for computing crop water requirements. FAO Irrigation and Drainage Paper n° 56. Food and Agriculture Organization of the United Nations

Apaydin H, Erpul G, Bayramin I, Gabriels D (2006) Evaluation of indices for characterizing the distribution and concentration of precipitation: a case for the region of Southeastern Anatolia Project, Turkey. J Hydrol 328: 726–732

Bonaccorso B, Bordi I, Cancielliere A, Rossi G, Sutera A (2003) Spatial variability of drought: an analysis of the SPI in Sicily. Water Resour Manag 17:273–296

Bordi I, Fraedrich FW, Gerstengarbe FW, Werner C, Sutera A (2004) Spatio-temporal variability of dry and wet periods in eastern China. Theor Appl Climatol 77:125–138

Burgueno A, Martinez MD, Serra C, Lana X (2010) Statistical distributions of daily rainfall regime in Europe for the period 1951–2000. Theor Appl Climatol 102:213–226

Capra A, Consoli S, Scicolone B (2013) Long-term climatic variability in Calabria and effects on drought and agrometeorological parameters. Water Resour Manag 27:601–617

De Luis M, Raventós J, Gonzalez-Hidalgo JC, Sánchez JR, Cortina J (2000) Spatial analysis of rainfall trends in the region of Valencia (East Spain). Int J Climatol 20:1451–1469

De Luis M, Longares LA, Stepánek P, González-Hidalgo JC (2007) Tendencias estacionales de la precipitación en la cuenca del Ebro (1951–2000). Geographicalia 52:53–78
De Luis M, Gonzalez-Hidalgo JC, Longares LA, Stepánek P (2009) Seasonal precipitation trends in the Mediterranean Iberian Peninsula in second half of 20th century. Int J Climatol 29:1312–1323
De Luis M, Gonzalez-Hidalgo JC, Longares LA (2010) Is rainfall erosivity increasing in the Mediterranean Iberian Peninsula? Land Degrad Dev 21:139–144
De Luis M, Gonzalez-Hidalgo JC, Brunetti M, Longares LA (2011) Precipitation concentration changes in Spain 1946–2005. Nat Hazards Earth Syst Sci 11:1259–1265
Del Río S, Herrero L, Pinto-Gomes C, Penas A (2011) Spatial analysis of mean temperature trends in Spain over the period 1961–2006. Global Planet Chang 78:65–75
Del Río S, Cano-Ortiz A, Herrero L, Penas A (2012) Recent trends in mean maximum and minimum air temperatures over Spain (1961–2006). Theor Appl Climatol 109:605–626
Domonkos P (2003) Recent precipitation trends in Hungary in the context of larger scale climatic changes. Nat Hazards 29:255–271
El Kenawi A, Lopez-Moreno JI, Stepanek P, Vicente-Serrano SM (2011) An assessment of the role of homogenization protocol in the performance of daily temperature series and trends: application to north-eastern Spain. Int J Climatol 33:87–108
El Kenawi A, Lopez-Moreno JI, Vicente-Serrano SM (2012) Trend and variability of surface air temperature in northeastern Spain (1920–2006): linkage to atmospheric circulation. Atmos Res 106:159–180
Elagib NA (2011) Changing rainfall, seasonality and erosivity in the hyper-arid zone of Sudan. Land Degrad Dev 22:505–512
Errasti I, Ezcurra A, Sáenz J, Ibarra-Berastegi G (2011) Validation of IPCC AR4 models over the Iberian Peninsula. Theor Appl Climatol 103:61–79
Espadafor M, Lorite IJ, Gavilán P, Berengena J (2011) An analysis of the tendency of reference evapotranspiration estimates and other climate variables during the last 45 years in southern Spain. Agric Water Manag 98:1045–1061
FAO (2002) Crops and drops. Making the best use of water for agriculture. Food and Agriculture Organization of the United Nations
FAO (2003) Unlocking the water potential of agriculture. Food and Agriculture Organization of the United Nations
García-Garizábal I, Causapé J (2010) Influence of irrigation water management on the quantity and quality of irrigation return flows. J Hydrol 385:36–43
García-Garizábal I, Causapé J, Abrahao R (2011) Application of the irrigation land environmental evaluation tool for flood irrigation management and evaluation of water use. Catena 87:260–267
González-Aparicio I, Hidalgo J (2011) Dynamically based future daily and seasonal temperature scenarios for the northern Iberian Peninsula. Int J Climatol 32:1825–1833
Gonzalez-Hidalgo JC, Lopez-Bustins JA, Stepánek P, Martin-Vide J, Luis M (2009) Monthly precipitation trends on the Mediterranean fringe of the Iberian Peninsula during the second-half of the twentieth century (1951–2000). Int J Climatol 29:1415–1429
Gonzalez-Hidalgo JC, Brunetti M, Luis M (2010) Precipitation trends in Spanish hydrological divisions, 1946–2005. Clim Res 43:215–228
Gonzalez-Hidalgo JC, Brunetti M, Luis M (2011) A new tool for monthly precipitation analysis in Spain: MOPREDAS database (monthly precipitation trends December 1945–November 2005). Int J Climatol 31:715–731
Guttman NB (1999) Accepting the Standardized Precipitation Index: a calculation algorithm. J Am Water Resour Assoc 35:311–322
Hayes M, Wilhite DA, Svoboda M, Vanyarkho O (1999) Monitoring the 1996 drought using the Standardized Precipitation Index. Bull Am Meteorol Soc 80:429–438
IPCC (2007) Climate change 2007: synthesis report. Contribution of Working Groups I, II and III to the Fourth Assessment Report of the Intergovernmental Panel on Climate Change [Core Writing Team, Pachauri RK and Reisinger A (eds)]. IPCC
IPCC (2008) Climate change and water. Cambridge University Press, Cambridge
IPCC-TGICA (2007) General guidelines on the use of scenario data for climate impact and adaptation assessment. Version 2. Prepared by T.R. Carter on behalf of the Intergovernmental Panel on Climate Change, Task Group on Data and Scenario Support for Impact and Climate Assessment
Kendall MG (1975) Rank correlation method. Griffin, London
Keyantash J, Dracup J (2002) The quantification of drought: an evaluation of drought indices. Bull Am Meteorol Soc 83:1167–1180

Lloyd-Hughes B, Saunders MA (2002) A drought climatology for Europe. Int J Climatol 22:1571–1592
Lopez-Moreno JI, Vicente-Serrano SM, Moran-Tejeda E, Zabalza J, Lorenzo-Laruz J, Garcia-Ruiz JM (2011) Impact of climate evolution and land use changes on water yield in the Ebro basin. Hydrol Earth Syst Sci 15:311–322
Loukas A, Vasiliades L (2004) Probabilistic analysis of drought spatiotemporal characteristics in Thessaly region, Greece. Nat Hazards Earth Syst Sci 4:719–731
Mann HB (1945) Nonparametric test against trend. Econometrica 13:245–259
Martínez-Cob A, Tejero-Juste M (2004) A wind-based qualitative calibration of the Hargreaves ET_0 estimation equation in semiarid regions. Agric Water Manag 64:251–264
Martins DS, Raziei T, Paulo AA, Pereira LS (2012) Spatial and temporal variability of precipitation and drought in Portugal. Nat Hazards Earth Syst Sci 12:1493–1501
McKee TBN, Doesken J, Kleist J (1993) The relationship of drought frequency and duration to time scales. Eight Conference on Applied Climatology. American Meteorological Society, Anaheim
McKee TBN, Doesken J, Kleist J (1995) Drought monitoring with multiple time scales. Ninth Conference on Applied Climatology. Am. Meteorol. Soc, Dallas
Milly PCD, Dunne KA, Vecchia AV (2005) Global pattern of trends in streamflow and water availability in a changing climate. Nature 438:347–350
Moratiel R, Durán JM, Snyder RL (2010) Responses of reference evapotranspiration to changes in atmospheric humidity and air temperature in Spain. Clim Res 44:27–40
Oliver JE (1980) Monthly precipitation distribution: a comparative index. Prof Geogr 32:300–309
Palatella L, Miglietta MM, Paradisi P, Lionello P (2010) Climate change assessment for Mediterranean agricultural areas by statistical downscaling. Nat Hazards Earth Syst Sci 10:1647–1661
Philandras CM, Nastos PT, Kapsomenakis J, Douvis KC, Tselioudis G, Zerefos CS (2011) Long term precipitation trends and variability within the Mediterranean region. Nat Hazards Earth Syst Sci 11:3235–3250
Pizarro R, Cornejo F, Gonzalez C, Macaya K, Morales C (2008) Analysis of rainfall behavior and aggressiveness in the central zone of Chile. Ing Hidraulica Mexico 23:91–109
Ramos MC (2001) Rainfall distribution patterns and their change over time in a Mediterranean area. Theor Appl Climatol 69:163–170
Ramos MC, Balasch JC, Martínez-Casanovas JA (2012) Seasonal temperature and precipitation variability during the last 60 years in a Mediterranean climate area of Northeastern Spain: a multivariate analysis. Theor Appl Climatol 110:35–53
Raziei T, Bordi I, Pereira LS (2008) A precipitation-based regionalization for Western Iran and regional drought variability. Hydrol Earth Syst Sci 12:1309–1321
Rouault M, Richard Y (2003) Intensity and spatial extension of droughts in South Africa at different time scales. Water SA 29:489–500
Sanchez-Arcilla A, Mösso C, Sierra JP, Mestres M, Harzallah A, Senouci M, El Raey M (2011) Climatic drivers of potential hazards in Mediterranean coasts. Reg Environ Chang 11:617–636
Saz Sánchez MA, López Martín F, Cabrera Mollet M, Cuadrat Prats JM (2007) Atlas climático de Aragón. Gobierno de Aragón, Servicio de Información y Educación Ambiental
Sen PK (1968) Estimates of the regression coefficient based on Kendall's tau. J Am Stat Assoc 63:1379–1389
Sneyers R (1992) Use and misuse of statistical methods for detection of climatic change. Climate Change Detection Project, Report on the Informal Planning Meeting on Statistical Procedures for Climate Change Detection
Turkes M, Tatli H (2009) Use of the standardized precipitation index (SPI) and a modified SPI for shaping the drought probabilities over Turkey. Int J Climatol 29:2270–2282
UN (2011) Global drylands: a UN system-wide response. United Nations Environment Programme (UNEP)
Vicente-Serrano SM, Cuadrat-Prats JM (2007) Trends in drought intensity and variability in the middle Ebro valley (NE of the Iberian Peninsula) during the second half of the twentieth century. Theor Appl Climatol 88: 247–258
Vicente-Serrano SM, López-Moreno JI (2006) The influence of atmospheric circulation at different spatial scales on winter drought variability through a semi-arid climatic gradient in northeast Spain. Int J Climatol 26: 1427–1453
Vicente-Serrano SM, Begueria S, Lopez-Moreno JI, Garcia-Vera MA, Stepánek P (2010) A complete daily precipitation database for northeast Spain: reconstruction, quality control, and homogeneity. Int J Climatol 30:1146–1163
Zargar A, Sadiq R, Khan FI (2014) Uncertainty-driven characterization of climate change effects on drought frequency using enhanced SPI. Water Resour Manag 28:15–40